Journal Pre-proofs

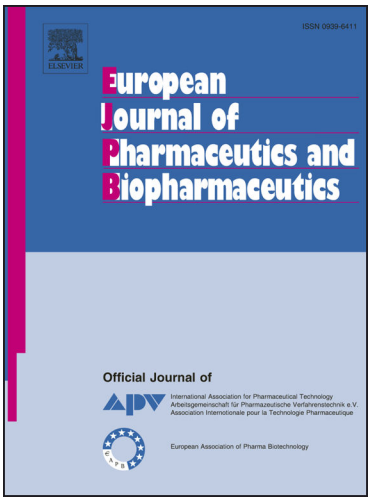

Dopamine-loaded lipid based nanocarriers for intranasal administration of the neurotransmitter: a comparative study

Adriana Trapani, Elvira De Giglio, Stefania Cometa, Maria Addolorata Bonifacio, Laura Dazzi, Sante Di Gioia, Md Niamat Hossain, Rosalia Pellitteri, Sophia G. Antimisiaris, Massimo Conese

PII: S0939-6411(21)00203-4
DOI: https://doi.org/10.1016/j.ejpb.2021.07.015
Reference: EJPB 13631

To appear in: *European Journal of Pharmaceutics and Biopharmaceutics*

Received Date: 11 November 2020
Revised Date: 9 July 2021
Accepted Date: 22 July 2021

Please cite this article as: A. Trapani, E. De Giglio, S. Cometa, M. Addolorata Bonifacio, L. Dazzi, S. Di Gioia, M. Niamat Hossain, R. Pellitteri, S.G. Antimisiaris, M. Conese, Dopamine-loaded lipid based nanocarriers for intranasal administration of the neurotransmitter: a comparative study, *European Journal of Pharmaceutics and Biopharmaceutics* (2021), doi: https://doi.org/10.1016/j.ejpb.2021.07.015

Dopamine-loaded lipid based nanocarriers for intranasal administration of the neurotransmitter: a comparative study

Adriana Trapani[a*], Elvira De Giglio[b], Stefania Cometa[c], Maria Addolorata Bonifacio[b], Laura Dazzi[d], Sante Di Gioia[e*], Md Niamat Hossain[e], Rosalia Pellitteri[f], Sophia G. Antimisiaris,[g] Massimo Conese[e]

[a]Department of Pharmacy-Drug Sciences, University of Bari "Aldo Moro", Bari, Italy

[b]Chemistry Department, University of Bari "Aldo Moro", via Orabona, 4, 70125 Bari, Italy

[c]Jaber Innovation s.r.l., 00144 Rome, Italy

[d]Department of Life and Environmental Sciences, Section of Neuroscience and Anthropology, University of Cagliari, Monserrato (Cagliari), Italy

[e]Department of Medical and Surgical Sciences, University of Foggia, Foggia, Italy

[f]Institute for Biomedical Research and Innovation (IRIB-CNR), 95126 Catania, Italy

[g]Laboratory of Pharm. Technology, Dept. of Pharmacy, School of Health Sciences, University of Patras, Rio 26504, Greece

[h]Foundation for Research and Technology Hellas, Institute of Chemical Engineering Sciences, FORTH/ICE-HT, Rio 26504, Greece

*Corresponding authors:

*A.T.: Email: adriana.trapani@uniba.it

*S.D.G.: Email: sante.digioia@unifg.it

Abstract

Both dopamine (DA) loaded Solid Lipid Nanoparticles (SLN) and liposomes (Lip), designed for intranasal administration of the neurotransmitter as an innovative Parkinson disease treatment, were already characterized *in vitro* in some extent by us (Trapani et al., 2018a and Cometa et al., 2020, respectively). Herein, to gain insight into the structure of SLN, X-ray Photoelectron Spectroscopy Analysis was carried out and DA-SLN (SLN 1) were found to exhibit high amounts of the neurotransmitter on the surface, whereas the external side of Glycol Chitosan (GCS) containing SLN (SLN 2) possessed only few amounts. However, SLN 2 were characterized by the highest encapsulation DA efficiency (*i.e.,* 81%). Furthermore, in view of intranasal administration, mucoadhesion tests *in vitro* were also conducted for SLN and Lip formulations, evidencing high muchoadesive effect exerted by SLN 2. Concerning *ex-vivo* studies, SLN and Lip were found to be safe for Olfactory Ensheathing Cells and fluorescent SLN 2 were taken up in a dose-dependent manner reaching the 100% of positive cells, while Lip 2 (chitosan-glutathione-coated) were internalised by 70% OECs with six-times more lipid concentration. Hence, SLN 2 formulation containing DA and GCS may constitute interesting formulations for further studies and promising dosage form for non-invasive nose-to-brain neurotransmitter delivery.

Keywords: *Liposomes, Solid lipid nanoparticles, Dopamine, X-Ray Photoelectron Spectroscopy Analysis, Cytotoxicity, Olfactory Ensheathing cells, Uptake.*

List of chemical compounds studied in the article: Dopamine hydrochloride (Compound CID: 65340), Chitosan (Compound CID: 129662530), Hydroxyethylcellulose (Compound CID: 4327536), Dimethyl Sulphoxide (Compound CID:679).

1. Introduction

Parkinson's disease (PD) is a neurodegenerative disorder that mainly affects older adults, particularly in economically developed Countries [1]. The PD patient typically shows alterations of body movements, including tremor, bradykinesia, and postural instability together with gastrointestinal symptoms [2]. The main PD pathological features are the loss of dopamine-generating neurons in the Substantia Nigra and Lewy bodies and abnormal protein aggregates including alpha-synuclein and ubiquitin in high extent in the brain [3-5]. Currently, the most followed therapeutic approach for PD involves the so-called "dopamine (DA) replacement strategy" which allows to control PD motor symptoms. In particular, levodopa (L-Dopa), still represents the most effective and reference drug [3, 5]. DA, indeed, cannot cross the Blood-Brain-Barrier (BBB) due to its physicochemical and metabolic features [4], whereas L-Dopa can overcome the BBB and is converted in the brain to DA by L-Dopa-decarboxylase mediated decarboxylation [4, 6, 7]. It should be noted that even in pathologies as stroke, PD, and Alzheimer's disease where the BBB is compromised and permeable enough, it still constitutes an obstacle to drug delivery into the brain [8, 9]. In this context, nanostructured drug delivery systems have demonstrated to be promising vehicles and, thus, most interest has been focused on the development of DA-loaded nanocarriers as an innovative approach for PD treatment [4, 10-14]. In addition, it has also been pointed out that the intranasal route of administration may constitute a useful approach for a non-invasive method of bypassing BBB supplying therapeutic agents into the brain [7, 15, 16]. Following this administration route, delivery of therapeutics to the brain occurs exploiting the connections between the olfactory epithelium located on the roof of the nasal cavity and the olfactory and trigeminal nerve components [7, 15, 16].

Apart from this, a challenging aspect in DA chemical manipulations is that, in the presence of molecular oxygen, DA undergoes a spontaneous autoxidation reaction under neutral/alkaline conditions. In such autoxidation process, the key steps are the aminochrome formation and the successive synthesis of polymer compounds (e.g., neuromelanins) through reactive oxygen species (ROS) which may be crucial in the development of neurodegenerative diseases as PD [17-19]. In this regard, it has been hypothesized that DA encapsulation in nanocarriers may reduce the autoxidation reaction of the same neurotransmitter [18]. Our interest for DA brain delivery by nanocarriers [4, 11, 12] led us to evaluate the protective effect toward the autoxidation reaction of DA encapsulation in liposomes. We found that both the uncoated and, in particular, the chitosan-glutathione (CS-GSH)-coated ones showed a prolonged stability against oxidative damage [18]. Definitively, DA-loaded nanocarriers administered by nasal route may represent an innovative and disease-modifying approach for PD treatment, because it may allow not only the BBB crossing and neurotransmitter sustained delivery but also may reduce the oxidative damage, leading to neuroinflammation. In

addition, it should be considered that advances in the preparative methods of nanomaterials allowed the availability of very small in size nanocarriers with interesting features including prolonged circulation, sustained release and BBB crossing [20-23].

Among the DA-loaded nanocarriers employed for PD treatment, mainly polymeric nanocarriers have been investigated [4, 11-14]. However, to the best of our knowledge, the potential of lipid-based nanocarriers for intranasal delivery of the neurotransmitter has not been deeply investigated. Lipid-based nanocarriers are at the forefront of the nanotechnology applied in drug delivery and especially for delivery to the brain [24]. Thus, for instance, liposomes are colloidal carriers extensively used, besides cyclodextrins [25] and polymeric micelles [26], to improve the formulation of hydrophobic drugs for their non-toxic, non-immunogenic, and biodegradable features. However, liposomes possess some drawbacks including the leakage of the encapsulated therapeutic molecule and the sensitivity of phospholipids to heat and radiation during sterilization processes. In recent years, solid lipid nanoparticles (SLN) have attracted increasing interest since their favorable features include safety and stability, controlled drug release, reduced leakage of the encapsulated drug for both hydrophobic and hydrophilic drugs [27]. Moreover, several routes of administration can be adopted for SLN supply, among which the oral one matches the patient compliance and the approval of the pharmaceutical industry [28, 29]. In the present work, to gain insights into the possible role played by lipid based nanocarriers in DA delivery to the brain by intranasal administration of the neurotransmitter, we report and discuss some results arising from the comparison of using DA-loaded liposomes and DA-loaded SLN. Overall, the aim of this study was to demonstrate what are the advantages/disadvantages of using DA-loaded liposomes or DA-loaded SLN for DA-replacement therapy.

Liposome formulation took place according to the Dried Reconstituted Vesicles (DRV) method using a mixture of phosphatidyl choline, phosphatidyl glycerol and cholesterol as lipid components following our previous work [18]. SLN were prepared following the melt homogenization method using Gelucire® 50/13, a self-emulsifying lipid, as lipid component taking into account that such lipid matrix was capable to increase the drug loading of hydrophilic active principles such as the neurotransmitter DA [30, 31]. From a chemical viewpoint, Gelucire® 50/13, is a mixture of PEG-esters (stearoyl polyoxyl-32 glycerides), a small glyceride fraction and free PEG chains, leading to a self-emulsify effect with aqueous media and, hence, the resulting SLN may be considered PEGylated SLN. Besides unmodified liposomes and SLN, the chitosan-glutathione conjugate (CS-GSH)-coated DA-loaded liposomes as well as Glycol Chitosan (GCS)-associated DA-loaded Gelucire® 50/13 SLN were also evaluated. Both CS-GSH coating and GCS association were employed as an approach to limit the immature leakage of the encapsulated neurotransmitter from liposomes and SLN,

respectively. The polycation GCS was preferred to the parent polymer CS for the higher aqueous solubility in neutral and physiological conditions [30]. Moreover, in view of intranasal administration, the DA-loaded nanocarriers were subjected to mucoadhesion and X-Ray photoelectron spectroscopy (XPS) studies and their cytotoxicity and uptake by glial cells involved in nose-to-brain delivery, namely Olfactory Ensheathing Cells (OECs), were also determined, as well.

2. Materials and methods

2.1. Materials

Dopamine hydrochloride, Cholesterol (Chol), Glycol chitosan, Fluorescein 5(6)-isothiocyanate (FITC), 6-Coumarin (6-COUM), carboxyl ester hydrolase (E.C. 3.1.1.1, 15 units/mg solid) from porcine liver, Tween® 85 were purchased from Sigma-Aldrich (Milan, Italy). According to the manufacturer instructions, Glycol chitosan was characterized by average molecular weight (M_n) of 400 kDa. Soybean phosphatidyl choline (PC, 70% of purity) and phosphatidyl glycerol (PG, 99.6% of purity) were provided by Lipoid (Germany). Gelucire® 50/13 was kindly donated by Gattefossè (Milan, Italy). Hydroxyethyl cellulose (HEC, Natrosol 250) was obtained by Aakon Polichimica (Milan, Italy). The polycarbonate filters for liposome extrusion (LiposoFast-Basic extruder) were purchased from Avestin (Germany). Chitosan-glutathione conjugate (CS-GSH) was prepared as previously reported [32]. For CS-GSH, M_n was determined to be equal to 49.4± 0.3.kDa [32].
For solutions and suspensions preparation, double distilled water was used. All other chemicals were of reagent grade.

2.2. Preparation of liposomes

The liposomes were prepared following DRV method as previously reported [18, 33]. Briefly, to obtain DA-unloaded liposomes, a mixture of PC/PG/Chol at 9:1:10 mol:mol:mol, respectively, [each dissolved in chloroform/methanol (2:1, v/v)] in a 50 mL round-bottom flask was evaporated by a rotary evaporator set at 40°C, leading to a thin-film formation. These lipid films were hydrated by addition of 10% (v/v) phosphate buffered saline (PBS, pH 6, 1 mM) at room temperature giving rise to plain Multilamellar Vesicles (MLVs) which were then reduced in size by probe sonication (at least two 10 min cycles of sonication were necessary) followed by a centrifugation step, (14000 rpm,6 min), providing so empty Small Unilamellar Vesicles (SUV). To prepare uncoated DA-loaded liposomes (Lip 1), an aliquot of 0.5 mL was withdrawn from a light protected aqueous DA solution in d-H_2O (10 mg/mL) and then mixed with 1 mL of the SUV liposomes. The resulting mixture was lyophilized overnight at −48 °C and 0.150 mBar pressure, and subjected to controlled re-hydration. Then, extrusion of the liposomes occurred through 400 nm and then 200 nm pore size polycarbonate

filters, by LiposoFast-Basic extruder and the resulting suspensions were ultracentrifuged. The precipitated purified liposomes were the uncoated DA-loaded liposomes.

To prepare the CS-GSH coated DA-loaded liposomes (Lip 2), the uncoated DA loaded vesicles were incubated with the coating solutions for 1 h under mechanical stirring at room temperature under light protection. The coating solution of CS-GSH was separately prepared dissolving a suitable amount of the polysaccharide at pH 4.4 in order to prepare a solution at 0.3 mg/mL concentration, which was stirred overnight at room temperature and then filtered through a 0.45 μm pore size filter. For uptake studies, fluorescent COUM-loaded Lip 1 and Lip 2 (*i.e.,* 6-COUM Lip 1 and 6-COUM Lip 2) were prepared following the same protocol above described with the following modifications. 10 mg of 6-COUM/mL of chloroform/methanol were employed instead of DA aqueous solution and they were added during thin-film formation.

2.3. SLN formulation

The preparation of DA-loaded Gelucire® 50/13 SLN (SLN 1) and GCS associated DA-loaded Gelucire® 50/13 SLN (SLN 2) was made following the melt homogenization method as previously reported [34]. Briefly, 60 mg-of the lipid Gelucire® 50/13 were melted at 70 °C and, in a separate vial, DA (10 mg), the surfactant (Tween® 85, 60 mg) and 1.37 mL diluted acetic acid, 0.01%, w/v, were mixed and, then, heated at 70 °C. To obtain an emulsion, the resulting aqueous phase was added to the melted fat phase at 70 °C and one cycle of homogenization was performed at 12300 rpm for 2 min with an UltraTurrax model T25 apparatus (Janke and Kunkel, Germany). Next, the nanosuspension was cooled at room temperature and the resulting SLN 1 centrifuged (16,000 × g, 45 min, Eppendorf 5415D, Germany) and the obtained pellet was re-suspended in distilled water for further studies.

To prepare the GCS-DA-SLN (SLN 2), 1.37 g of a previously formed solution of GCS (5 mg/mL in AcOH 0.01, w/v) was added to the aqueous phase containing DA (10 mg), the surfactant (Tween® 85, 60 mg) and 1.37 mL of water. Working up as reported above for SLN 1 the required SLN 2 were obtained. Control SLN were either the ones without both DA and GCS (namely, plain SLN) or the ones without DA, but containing GCS (namely, GCS-SLN). In view of biological experiments, fluorescent SLN (i.e., FITC-SLN) were prepared following the same protocol of GCS-DA-SLN, but replacing 10 mg of DA in the aqueous phase with the same amount of FITC.

2.4. Physicochemical characterization of lipid carriers

The determination of DA and 6-COUM were carried out by HPLC and fluorimetric assays, respectively, as previously reported [18, 35].

For liposomes and SLN, particle size and polydispersity index (PDI) were acquired by ZetasizerNanoZS (ZEN 3600, Malvern, UK) apparatus according to photon correlation spectroscopy (PCS) mode. The particle size of liposomes was measured at 25 °C after dilution with PBS (pH 6) to give a 0.4 mg/mL of final lipid concentration, whereas in the case of SLN the particle size and PDI was measured after dilution 1:1 (v:v) with double distilled water. For evaluation of zeta-potential of liposomes, measurements were performed at 25 °C (ZetasizerNanoZS, ZEN 3600, Malvern, UK) after dilution at the same concentration employed for size analysis in potassium phosphate buffer medium. Zeta average values were used for PCS analysis of SLN and liposomes herein described. In the case of SLN the zeta-potential was determined after sample dilution 1:20 (v:v) with KCl (1 mM, pH 7) [36, 37]. Ten replicates of size measurements and ten replicates of zeta potential values were reported for SLN and liposomes under investigation. For visualization of SLN 1 and SLN 2, a cryogenic transmission electron microscopy (Cryo-TEM) apparatus was adopted as already reported [38]. All observations were performed using a Hitachi 7700 electron microscope, setting the temperature at 105 K and the acceleration voltage at 100 KV. The instrument was equipped with a Gatan 626 cryo holder and digital microphotographs were acquired with an AMT-XR-81 camera and processed with the EMIP software.

2.5. *Physical stability of SLN formulations*

For SLN 1 and SLN 2 the physical stability was evaluated measuring their particle size after incubation upon storage at 4° C up to 2 months as well as monitoring the neurotransmitter content in the particles over the time.

For DA content monitoring, freshly prepared samples of SLN 1 and SLN 2 were centrifuged (16,000 × g, 45 min, Eppendorf 5415D, Germany) and the resulting pellets were re-suspended in distilled water and freeze-dried for 72 h (T = -46 °C and P = 0.1 mBar, Lio Pascal 5P, Milan, Italy). Then, the physical stability of the collected powders was evaluated upon storage at 4°C at different time intervals up to two months.

To evaluate the neurotransmitter content in the particles at different time points, at the end of prefixed storage time, appropriate aliquots of SLN were incubated with 1 mL of carboxyl ester hydrolase solution (0.6 mg/mL phosphate buffer pH 5.0) [36] at 37 °C for 30 min and, afterwards, centrifuged as described in Section 2.3. The obtained supernatant was analyzed by HPLC to determine the DA contents [18].

2.6. In vitro evaluation of mucoadhesive properties of DA liposomes and SLN

The mucoadhesive properties of DA-loaded liposomes and SLN were evaluated in Simulated Nasal Fluid (SNF) by turbidimetric measurements [32]. SNF was prepared after dissolution of $CaCl_2\ 2H_2O$ (0.32 mg/mL), KCl (1.29 mg/mL) and NaCl (7.45 mg/mL) in water at pH values in the range 5-6 [39].

To 6 mL of freshly prepared mucin dispersions in SNF (1 mg/mL) held in a water bath (Julabo, Milan, Italy) at 37 °C under stirring (150 rpm), freeze dried SLN (or liposome) formulations, previously dispersed in 6 mL of SNF, were added. The turbidity of the stirred mixture at 37 °C was measured at 0, 2, 5, 7 and 24 h at the wavelength of 650 nm using a Perkin-Elmer Lambda Bio 20 spectrophotometer and compared with that of HEC dissolved in SNF (0.4 mg/mL) and taken as positive control. Each experiment was performed in triplicate and the results are expressed as mean ± standard deviation of each mean.

2.7. X-Ray photoelectron spectroscopy (XPS) analyses performed on SLN

The SLN specimens, as well as the feed materials, were studied by means of the PHI 5000 VersaProbe II scanning microprobe (ULVAC-PHI, Minnesota). The instrument was provided with a monochromatized AlKα X-ray source. The measurements were carried out in HP mode, scanning a spot of ~ 1400 × 200 μm). Each sample analysis consisted in the acquisition of high-resolution spectra (acquired in FAT mode, pass energy 29.35 eV) and survey scans (binding energy (BE) range 0–1200 eV, FAT mode, pass energy 117.4 eV). Quantification (atomic percentage, At%) was performed on peak areas, once normalized by means of sensitivity factors from MultiPak library. The latter were also exploited to compare data belonging to different elements. Peak deconvolution has been done by MultiPak Data Reduction software (PHI), version 9.9.0). The charge reference (i.e., C1s adventitious carbon) was set at 284.8 eV.

2.8. Cytotoxicity studies with Olfactory Ensheathing Cells (OECs)

OECs were obtained from olfactory bulbs of mouse P2 as formerly reported [40, 41]. After plating on 25 cm^2 flasks, the cells were grown in Dulbecco's Modified Eagle's medium (DMEM) supplemented with 10% FBS and bovine pituitary extract, with regular media changes twice a week. Subsequently, cells (3×10^4 cells/well) were seeded in 96-well plates and exposed to either plain SLN (0.25, 0.5, 1, 2.5, 5, and 10 μg/mL of lipids) in complete medium, or DA-SLN, or GCS-DA-SLN (same lipid concentrations corresponding to DA concentrations of 0.45, 0.9, 1.8, 4.5, 9.0. and 18 μM), or liposomal formulations Lip 1 and Lip 2 (0.25, 1, 4, 16, and 64 μg/mL of lipids, corresponding to DA concentrations of 0.3, 1.17, 4.7, 9, 18.75, and 75 μM). Twenty-four h after treatments, cell

viability was evaluated by MTT (3-(4,5-dimethylthiazol-2-yl)-2,5 diphenyl tetrazolium bromide), as previously described [4]. The cell viability was calculated as follows: % viability = [(Optical density {OD} of treated cell − OD of blank)/(OD of vehicle control − OD of blank) × 100], considering untreated cells as 100%. Cells treated with 1% Triton X-100 were used as positive control.

2.9. Uptake studies

OECs (5×10^4 cells/well) were grown in a 24-well culture plate for 1 day. Cells treatments were carried out with FITC-SLN (0.25-10 μg/mL of lipids) or 6-COUM-liposomal formulations (0.25-64 μg/mL) in complete medium. After 24 h, cells were treated with trypan blue (0.04% in PBS) in order to quench extracellular fluorescence. Afterwards, cells were trypsinized, resuspended in PBS, and analysed by Amnis Flowsight IS100 (Merck). After brightfield scatter plots obtained by plotting Area on x-axis vs Aspect Ratio on y-axis were generated, single cells events were gated, and finally 10,000 single-cell events for sample were acquired. The percentage of green positive cells (channel 2, 488 nm excitation laser) and mean fluorescence were analysed using Amnis IDEAS software [42].

2.10. Statistical analysis

Statistical analyses were carried out by Prism v. 4, GraphPad Software Inc., USA. Data were expressed as mean ± SD. Multiple comparisons were based on one-way analysis of variance (ANOVA) with the either Bonferroni's or Tukey's post hoc test and differences were considered significant when $p < 0.05$.

3. Results

In Table 1 the main physicochemical features of DA-loaded liposomes and SLN are summarized. Among others, it can be deduced from Table 1 that DA-loaded CS-GSH coated liposomes (Lip 2) showed a mean diameter lower than the corresponding uncoated vesicles (Lip 1). Such significant size decrease has been accounted for the three different extrusion treatment through cut-off membrane filters used for the former vesicles preparation, unlike the latter ones [18]. Moreover, SLN 2 exhibited a significant size reduction compared to the control ones (i.e., GCS-SLN) and this result was ascribed to the capability of GCS to undergo a conformational reorganization in the presence of the neurotransmitter, leading to GCS-DA-SLN shrinkage [34]. However, the most relevant finding was the higher E.E.% observed for SLN compared with the liposome formulations, particularly when SLN

2 is considered for which an E.E.% of 81% was observed. The PDI values of DA-loaded liposomes and SLN were found in the range 0.16-0.27 indicating, on the whole, a narrow size distribution while, in the case of SLN 2 and respective control SLN, the PDI values were higher implying a broader size distribution. Except for Lip 1 and control SLN, the zeta potentials of the investigated formulations were low in absolute value, whereas the introduction of the polycationic materials represented by CSGSH and GCS for liposomes and SLN, respectively, induced a positive surface charge (Table 1). Moreover, for SLN 2, TEM microphotograph (Fig. 1c) evidenced a good agreement with particle size determined via PCS approach and, in comparison to the compact round shaped SLN 1 (Fig 1 a and 1b [38]), SLN 2 appeared slightly distorted round shaped.

[Insert Figure 1 and Table 1]

Overall, further physicochemical characterizations of liposomes and SLN nanocarriers herein studied, including physical and oxidative stability of vesicles as well as the infrared spectroscopy in attenuated total reflectance mode (FT-IT/ATR) and thermogravimetric analyses (TGA) of SLN are reported in ([18] and [34]) to which the reader is referred to.

3.1. Stability studies on DA-loaded liposomes and SLN

We have previously studied the stability of Lip 1 and Lip 2 in terms of DA content over the time and temperature dependence and the extent of the autoxidation of the neurotransmitter was also investigated [18]. Within six days of storage at 22 °C and 4 °C, Lip 2 were found to be more stable than Lip 1 at both tested temperatures. Probably, such greater oxidative stability should be ascribed to the localization of the neurotransmitter in the core of these nanocarriers but not on their surfaces as proved by XPS studies [18]. In addition, it could be also due to the CS-GSH thiomer coating layer which can prevent DA degradation thanks to the antioxidant role of GSH [18].

The low zeta potential in absolute values observed for DA-loaded liposomes and SLN suggested that an in-depth study on the physical stability of both formulations was mandatory. While such a study has already been reported for the vesicle formulations suggesting that Lip 2 is stable against oxidative damage up to 6 days of storage [18], herein, physical stability of SLN in the presence and in the absence of GCS was assessed at 4 °C, evaluating both particle mean diameter and neurotransmitter content evolution over the time. As reported in Fig. 2a, SLN 2 underwent to significant particle size decrease at the latest time points ($p<0.001$), whereas SLN 1 mean particle size was kept constant up to 1 month and, afterwards, particle size markedly increased ($p<0.001$) together with grey-black precipitate formation, indicative of particle aggregation and autoxidation of the active DA. Concerning DA content in SLN 2, it was essentially equal to the starting value within 2 weeks but,

after 1 month of storage, half of the original DA amount was found ($p<0.001$) (Fig. 2b). The same trend in DA content was observed for SLN 1 even if the decrease in neurotransmitter amount at longer exposure times was lower than that observed for SLN 2. By comparing the SLN formulations with the vesicle Lip 1 and Lip 2 ones, it seems that the former preparations possess a greater physical stability. In particular, SLN 2 appear promising in terms of storage since their mean diameter and DA content can be maintained essentially constant for two weeks. Moreover, it is noteworthy that only after three months of storage at 4 °C, a change to pale grey colour of SLN 2 freeze-dried powders was noted by visual inspection, suggesting chemical (oxidative and hydrolytic) degradation is starting. Probably, the higher physical stability of SLN 2 formulation should be due to the localization of the neurotransmitter inside the nanocarrier and this feature is expected to safeguard it from chemical degradation for a longer time [18].

[Insert Figure 2]

3.2. Mucoadhesive properties of DA-loaded liposomes and SLN

In view of the *in vivo* administration through the nasal mucosa, the *in vitro* mucoadhesive properties of DA containing liposomes and SLN were assessed by turbidimetric measurements carried out in SNF. Indeed, once DA-loaded liposomes- and SLN-mucin aggregates are formed by mixing each mixtures of these nanocarrier suspensions with mucin dispersion in the same medium, then a decrease in transmittance percentage occurs depending on the incubation time [43]. For these experiments, powders of freeze-dried liposomes and SLN were directly dispersed in SNF and the changes in transmittance at 650 nm wavelength were recorded, comparing the results with those of HEC included as positive control. HEC, indeed, possesses good mucoadhesive characteristics, even though lower than Carbopol 974P [44] which, on the other hand, could not be employed due to its precipitation in SNF under conditions we used. Furthermore, after visual inspection, no change in colour of the tested formulations throughout the study was observed and it suggests that no chemical (oxidative and hydrolytic) degradation occurs. As shown in Fig. 3 among all tested formulations Lip 2 and SLN 1 showed mucoadhesive properties similar to the one of HEC. Interestingly, the most relevant reduction decrease in transmittance after 24 h of incubation time was observed for SLN 2 followed by Lip 1 which both resulted in statistically significant difference compared with control ($p<0.001$ and <0.01 *vs* HEC, respectively).

Hence, based on the turbidimetric measurements after 24 h incubation time, the observed rank order of mucoadhesive properties for the examined formulations is the following: SLN 2 > Lip 1 > SLN 1, Lip 2 > HEC and, in particular, the most mucoadhesive formulation resulted SLN 2.

[Insert Figure 3]

3.3. XPS studies

XPS analysis of the SLN, with or without GCS and DA, was carried out to provide clues on the chemical composition of the surface as well as on the possible modifications or interactions between the different components within the investigated formulations. The pure neurotransmitter and all the SLN components were analyzed as well. In Table 2 the elemental atomic percentages recorded on the surface of each sample are summarized. As for the XPS analyses of Lip 1 and Lip 2 formulations, they were previously reported and discussed [18]. The curve fit of C1s belonging to the pure SLN components were reported in Figure 4.

As far as DA C1s signal is concerned (Fig. 4a), two components have been used to fit the signal: one at 284.8 eV, representing the C-C, C=C and C-H groups (plus contamination) and one at 286.3 eV, typical of C-OH and carbon linked to and ammonium salts. The peak ratio was found to be 1.7:1, in total agreement with that expected from the stoichiometry of dopamine molecule. For GCS (Fig. 4b), four contributions were detected on carbon signal. In particular, the first at 284.8 eV was peculiar of CHx compounds (plus contamination); the other peak, at 285.4 eV, was typical of amine groups; the third at 286.4 eV, was relevant to C-OH and C-NH_3^+ groups and finally the fourth peak, falling at 287.9 eV, was ascribable to the carbohydrates O-C-O linkage. The two components of SLN formulations, i.e., Gelucire 50/13 and Tween 85 (Figs 4c and 4d), presented both a five-peak C1s curve fitting, with different relative abundances, in agreement with the molecular formulas of these organic compounds. Precisely, hydrocarbon peak at 284.8 eV, a peak in α-position to a carboxylic group at 285.4 eV, an alcoholic peak at 286.3 eV, a carbonyl group at 287.3 eV and a carboxylic one at 288.8 eV were detected. Moreover, C1s signals relevant to plain SLN and SLN 2 formulations were curve-fitted and shown in Figs 4e and f, respectively, evidencing no additional contributions to the curve-fitting with respect to those present in the feed materials, although in different relative abundances. Overall, based on the higher neurotrasmitter E.E.% and physical stability, the better mucoadhesion performance and the sustained release without burst effect [30, 34]. SLN 2 was identified as the most interesting formulation for nose-to-brain DA delivery worthy of deeper *in vitro* and *ex vivo* studies.

[Insert Table 2 and Figure 4]

3.4. MTT studies on OECs

Since these SLN formulations are potentially designed for nose-to-brain delivery, their cytotoxicity on OECs was evaluated. Cell viability, by MTT, was determined 24 h after incubation of cells with plain SLN (not coated with GCS and not loaded with DA), SLN 1, or SLN 2. As shown in Fig. 5a, plain SLN were slightly toxic to OECs only at 5 and 10 μg/mL with a reduction of cell viability of around 20%. Interestingly, when compared with untreated cells (control) both SLN 1 and SLN 2 did not show any toxicity onto OECs at any concentration tested (Fig. 5b and 5c).

[Insert Figure 5]

Liposomal formulations were tested by the same assay and at the same time point. It is worth to consider that lipid concentrations are different from those present in SLN 1 and SLN 2 in order to obtain similar DA concentrations. However, Lip1 and Lip2 were not toxic to OEC cells, at tested lipid concentrations (Fig. 6).

[Insert Figure 6]

3.5. Uptake studies by OECs

Given the highest mucoadhesion properties presented by SLN 2, FITC-SLN 2 were prepared for uptake studies. Cell uptake of these formulations was evaluated in OECs following incubation for 24 h. Fig. 7a shows that the FITC-SLN 2 were internalised by an increasing percentage of cells, reaching the 100% at 5 μg/mL. This behaviour was paralleled by the increase in the mean fluorescence intensity (Fig. 7b). Altogether, these results are indicative of an internalisation of SLN by OECs mediated by a dose-response process.

[Insert Figure 7]

Uptake studies were also performed with liposomal formulations. Uncoated liposomes (Lip 1) were internalised in a dose-dependent manner obtaining only 9.0 ± 3.9% of positive cells at 16 μg/mL and, to further test the cell uptake capability of these liposomes, 27 ± 12.5% of positive cells with four-times higher concentration (64 μg/mL) (Fig. 8a), while the mean fluorescence intensity peaked already at 4 μg/mL (Fig. 8b). Interestingly, the coated formulation (Lip 2) was internalized by around 71% of cells with the highest lipid concentration (Fig. 8c), and with 1 μg/mL and above the mean fluorescence intensity was consistently higher as compared to the lowest concentration (Fig. 8d). Of note, the highest concentration (64 μg/mL) was not toxic to OECs (Fig. 5).

[Insert Figure 8]

4. Discussion

In the present work, DA-loaded-liposomes and -SLN were investigated in a comparative manner to evaluate their feasibility for neurotransmitter delivery to the brain by intranasal administration. For this purpose, in the first step of the study, attention was paid to the preparative aspects consisting in maximizing the encapsulation efficiency of the neurotransmitter in each of these nanocarrier types. While it is well known that hydrophilic substances as DA can be encapsulated in liposome aqueous core, in the case of SLN the encapsulation of water-soluble drugs, such as therapeutic peptides/proteins, is characterized by a low loading efficiency, mainly due to the leakage of the drug during nanoparticle preparation [45]. Thus, encapsulation of hydrophilic compounds in SLN is not a simple task and, indeed, it constitutes a challenge for scientists involved in the field. On the other hand, even liposome formulations may undergo drug leakage due to change of phospholipid bilayer integrity consequent to oxidation and chemical hydrolysis of phospholipids occurring in aqueous medium [27, 46]. It seems that an appropriate polymer coating (e.g. chitosan, alginate) may limit such drug leakage from vesicle formulations [47]. The most employed approach for an acceptable preparation of SLN loaded with a hydrophilic is the double emulsification (W/O/W) method endowed with, however, both a toxicological issue related to the use of organic solvents and tendency of globules to coalesce, so giving an increase in nanoparticle size [31]. In this regard, we are involved in demonstrating that the adoption of a self-emulsifying lipid in the melt homogenization method for SLN preparation, could represent a simple and alternative approach to double emulsification (W/O/W) method devoted to the formulation of hydrophilic drug-loaded SLN with satisfactory loading efficiency [31]. It follows from the hypothesis that, being a nano-emulsion formed once the self-emulsifying lipid is in the presence of water, the hydrophilic compound may be entrapped in the nano-emulsion, but its diffusion towards the aqueous external phase and the consequent leakage may be limited after the quick lipid recrystallization consequent to the cooling process. We have shown the feasibility of this approach in the encapsulation of the antioxidant tripeptide glutathione and the grape seed extract proanthocyanidins for which E.E.% up to 82.7 % was found for the former [34] and a loading efficiency equal to 5.8% (comparable with that calculated for the encapsulation of proanthocyanidins in a hydrophilic matrix as chitosan) was observed for the latter [42].

In the case herein examined of the neurotransmitter DA encapsulation in liposomes and SLN, data in Table 1 clearly show that vesicle formulations lead to unsatisfactory encapsulation efficiency even using DA-loaded CS-GSH coated liposomes (Lip 2) (*i.e.,* 12.2 ± 0.3%) and, hence, a polymer coating

of vesicles provided only a limited benefit. On the other hand, the E.E.% of SLN 1 was higher than that of Lip 2 resulting of 19 ± 3% which markedly increased to 81 ± 2 % when SLN 2 were examined. Hence, this positive result obtained with the hydrophilic neurotransmitter DA further supports the suggestion that SLN based on self-emulsifying lipid as Gelucire® 50/13 may be used to encapsulate hydrophilic compounds with satisfactory loading efficiency. Moreover, in this preparative approach, the association of the polycation GCS to DA-loaded Gelucire® 50/13 SLN seems most advantageous and it should be considered for a further increase the E.E.% of hydrophilic substances. This finding is also interesting if compared with the recent result reported in ref [48] where DA-loaded SLN made of glycerol tripalmitin/octadecylamine are described with an encapsulation efficiency at most of 70% and a lower storage stability (*i.e.,* 30% loss of DA content after a storage period of one week at 4 °C in the better case; [48]).

Concerning the findings of the mucoadhesion study on lipid formulations herein evaluated, the best mucoadhesive performance was observed for SLN 2. This result may be explained on the basis of the zeta potential recorded for these nanocarriers which, even though slightly positive, should allow electrostatic interactions with negatively charged mucus proteins leading to efficient adhesion [32]. Such zeta potential value of SLN 2 should be related to the association of polycation GCS whose good mucoadhesive performance are known [32, 49, 50]. Moreover, it should be also considered that GCS may be cross-linked giving rise to hydrogels which could be appropriately tailored from the pores size point of view by varying the degree of crosslinking [51, 52]. Hence, among the examined formulations, in the nasal cavity SLN 2 should better interact with mucus and increase residence time facilitating absorption [15]. The significant mucin interaction of negatively charged uncoated DA-loaded vesicles Lip 1 greater than the corresponding coated ones with CSGSH (Lip 2) is somewhat surprising if we consider that the high mucoadhesive properties of thiomers as CSGSH [32]. However, it should be also taken into account that, on the basis of XPS study previously carried out on these liposomes, it was evidenced that the -SH groups of the thiomer CS-GSH are not exposed outside the vesicles since no sulfur was detected on the surface [18]. Therefore, the thiol-disulfide exchange reactions with mucus protein chains responsible of improved mucoadhesive properties of thiomers should be reduced or absent at all, explaining so the lower mucoadhesion of Lip 2 compared with Lip 1 [18, 32].

The most interesting results deduced from XPS studies are summarized in Table 2. As shown, on GCS-SLN control, no nitrogen was detected, suggesting that GCS was not present on the surface. On the other hand, the N1s atomic percentages in SLN 1 and SLN 2 were quite similar, even if their E.E.% were significantly different, as already reported [34]. However, since XPS studies only the

surface composition of the samples, the similar nitrogen percentage is an indirect evidence of the drug massive presence in the internal layers, especially SLN 2, as highlighted by E.E.% data.

As far as DA C1s signal is concerned (Fig. 4a), the C-H_x/C-OH peak ratio was found to be 1.7:1, in total agreement with that expected from the stoichiometry of dopamine molecule. In GCS (Fig. 4b), the C-NH_2/O-C-O peak ratio was 0.96:1, indicating an almost totally neutral state of the bare macromolecule. In Gelucire 50/13 (Fig. 4c), the COH/COOR corrected area ratio was found to be 7:1, while in Tween 85 (Fig. 4d), the same ratio was 12:1. In the case of plain SLN (Fig. 4d), the C1s curve fitting was found to be the result of the combination of both Gelucire 50/13 and Tween 85 contributions, in agreement with that already reported [21]. Indeed, the COH/COOR was found to be 10:1. On the other hand, the presence of GCS in SLN 2 did not change the C1s curve fitting (Fig. 3f), as also verified in C1s signal relevant to GCS-SLN surface (Fig. 1S). Indeed, no O-C-O contribution, typical of GSC, was detected, indicating no allocation of GCS on the nanoparticle surface, irrespectively from the DA presence in the formulation. On the other hand, a huge C-OH peak increase (with a COH/COOR ratio equal to 24:1) was recorded on SLN 2 surface. This could be probably ascribable to a surface enrichment in Tween, but the presence of dopamine, with C-OH and C-NH_3^+ groups falling both at 286.3 eV, cannot be excluded. Actually, the DA presence on surface was also confirmed by the detection of the N1s signal. As far as SLN 1 is concerned, the C1s curve fitting resulted quite similar to that of SLN 2 (Fig. 2S). In addition, the nitrogen atomic percentages in SLN 1 and SLN 2 resulted comparable (Table 2), even if the encapsulation efficiency percentage (E.E. %) and the *in vitro* release of DA from these systems, already reported [34], resulted significantly different. All these findings let us to argue that in the SLN 2 nanocarriers, differently from the SLN 1, the neurotransmitter was not located on surface except for a negligible amount but encapsulated in the internal layers of the nanoparticles, leading to a very promising DA reservoir system. Moreover, the slightly positive zeta potential recorded for SLN 2, indicative of a surface GCS presence, was apparently in contrast with XPS evidences but it cannot be ruled out that in the wet physical state, where zeta potential measurements are performed, it can happen a partial rising of the GCS chains to the surface. This finding was not observed by XPS since in this technique particles were not examined in liquid suspension but at solid dry state [53].

The findings of these studies could be interpreted in the context of the model proposed by us for PEGylated SLN as the Gelucire® 50/13-based SLN [30]. Indeed, following a literature hint about PEG2000−stearic acid based SLN structure [54], we suggested that Gelucire® 50/13-based SLN consist of a hydrophilic shell of polyoxyethylene chains of solid lipid (Gelucire® 50/13) and cosurfactant (Tween 85) together with an internal lipid core where the stearoyl moieties are mainly present (Fig. 9a) [30]. This implies that a hydrophilic substance as the neurotransmitter DA, could be

adsorbed on the particle surface or entrapped in the hydrophilic shell as well as encapsulated in the lipid core as nano-emulsion and this is the case of SLN 1 formulation *i.e.,* the so called outer-shell distribution [55]. However, in such circumstances, some neurotransmitter adsorbed on the particle surface or entrapped in the hydrophilic shell could be lost for instance during sample manipulations which could reduce the corresponding E.E.%. When these PEGylated SLN were associated to GCS, this polycation should be placed inside the nanoparticles since on GCS-SLN control no nitrogen was detected by XPS analysis (Table 2). More precisely, the polycation should be placed within the hydrophilic shell because only in this layer formation of a network compact structure could occur arising from hydrogen bonding and polar interactions between the polyoxyethylene chains of Gelucire® 50/13 and GCS (Fig. 9b). In the case of SLN 2 formulation, besides in the lipid core as nano-emulsion, the neurotransmitter DA should be localized in the hydrophilic shell due to hydrogen bonding and polar interactions involving the polyoxyethylene chains, GCS and the functional groups of DA. In this last case, however, the presence of the mentioned network could limit the leakage of DA localized in the hydrophilic shell accounting for the marked increase in E.E.% observed for SLN 2 compared with SLN 1. In short, formation of the mentioned network structure in SLN 2, but not in SLN 1, accounts for the marked increase in E.E.% since the leakage of the neurotransmitter entrapped in internal layers in the former formulation should be hindered. Moreover, formation of the mentioned network structure could also explain the greater physical stability of SLN 2 compared with SLN 1 since it allows the localization of the neurotransmitter inside, but not on the surface of the nanocarrier for a longer time. However, it should be taken into account that, as far as the structures of the particles is concerned in SLN, further aspects remain to be clarified, including the arrangements of the lipids and stabilizing agents during the particles formation [55]. Overall, the model proposed for the Gelucire® 50/13-based PEGylated SLN could be also useful to interpret the results of *in vitro* release studies [18, 34].

[Insert Figure 9]

It is worth noting that plain SLN were quite toxic at high concentrations of lipid, whereas those SLN containing DA (both SLN 1 and SLN 2) were not. DA has been shown to reduce ferroptosis in cancer and non-cancer cells and increase cell viability at 12-5-50 μM by reducing glutathione depletion and malondialdehyde production [56]. Of note, some studies have reported a cytoprotective effect of L-DOPA, e.g. by inducing the synthesis of GSH in cultured cells [56, 57], suggesting a role of DA against oxidative stress, although we have not ruled out these events in our experimental conditions. It has been also found that DA increased proliferation of subventricular zone-derived cells inducing the release of EGF [58], an effect that could take part in its cytoprotective role in OECs. Concerning

uptake studies, in the literature, fluorescent polymersomes of PEG-PLGA have been already loaded with 6-COUM to investigate brain delivery in mice and, therefore, we selected the same probe 6-COUM in order to have affinity for the lipophilic vesicles, being 6-COUM a hydrophobic dye [59]. Interestingly, liposomal formulations seem to be less efficient than SLN in the uptake process, and the uncoated ones the lesser than the uncoated, although the mean fluorescence intensity reached similar levels considering all the SLN and liposomal nanoparticles. With four-times higher concentration, the coated liposomal formulation Lip 2 reached around 70% of positive cells. Overall, these results indicate that, in face of a similar average entry of fluorescent formulations, it is the number of cells that varies so that SLN can deliver DA in all the cells which they come into contact with at lipid concentrations lower than liposomes. Moreover, it is also suggested that delivering DA via the olfactory route with SLN would be more efficient than using liposomes. The main uptake mechanisms of nanocarriers are clathrin-mediated endocytosis (CLME), caveolae-mediated endocytosis (CVME) and macropinocytosis (MP), which can be used at variance with the cell line. Most of lipid-based nanoparticles are endocytosed via CLME, nevertheless several other pathways, like CVME and other dynamin-dependent processes can be involved [60]. For example, PEGylated SLN were shown to be taken up by oral squamous carcinoma cells through CLME [61]. Recent studies in excised olfactory mucosa have determined that the uptake of 150 nm SLN was unaffected by chlorpromazine, a CLME inhibitor, while it was significantly reduced but not abolished by amiloride, a MP inhibitor, indicating that various energy-dependent endocytic mechanisms may operate in the olfactory tissues [62]. However, the relationship between in-vitro, ex-vivo and in-vivo uptake by physiological cell types in different tissues remains to be further explored and is one of the major topics in the future nanotechnology agenda [63]. Depending on the uptake route, the fate of lipid-based nanocarriers can be different, thereby leading to evasion from lysosomal degradation and release from the cell via extracellular vesicles/exosomes [64, 65]. As a result, further distribution of the drug-loaded nanoparticles to more distant tissues can be achieved. In the context of nose-to-brain delivery, the uptake of SLN and liposomes by OECs could drive DA release in the perineural spaces, so to be transported to the olfactory bulb via either the paracellular pathway or the axonal transport after neuronal uptake, being likely a combination of the two transport mechanisms [15, 66].

The lack of cytotoxicity observed with DA-containing SLN highlights a safe delivery of this molecule through the olfactory region of nasal cavity. First of all, the mucoadhesive properties would reduce the mucociliary clearance of the drug in the vestibular region of the nose. In the posterior region of nasal cavity, the transport of the DA-containing nanoparticles would occur following different routes to the brain, among which of interest is the interaction with the endings of olfactory receptor neurons.

They will then pass the cribriform plate and enter into the cerebrospinal fluid and olfactory bulb through the nerve channel created by OECs enclosing the olfactory axons [67]. SLN 2, endowed with the highest mucoadhesion properties, were also taken up with high efficiency by OECs (reaching the 100% of positive cells), making possible to consider DA transport to the brain via OECs a safe way.

5. Conclusions

DA-loaded SLN 1 and SLN 2 have been investigated, in comparison with DA-loaded vesicles Lip 1 and Lip 2, to test the potential of these lipid nanocarriers for DA-replacement therapy in Parkinsonian patients following non-invasive nose-to-brain delivery approach. The high E.E.% observed for SLN 2 (81%), their better physical stability in terms of storage (*i.e.,* mean diameter and DA content essentially constant for two weeks) combined with their good mucoadhesion properties and lack of cytotoxicity towards OECs make these PEGylated nanocarriers as interesting candidates for further studies in comparison with the alternative lipid formulations (*i.e.,* SLN 1 and Lip 1 and Lip 2). Overall, this study demonstrates that it should be advantageous to use SLN 2 formulations for DA-replacement therapy.

Acknowledgements

This work was partially financed by University of Bari (Italy) to A.T. (Cod. CUP:H91J11000160001). A.T. would also acknowledge Dr. Tatiana Brenna (Gattefossè, Italy) for providing Gelucire® 50/13 lipid and Dr. Francesca Curci and Dr. Licia Anna Pugliese for their valuable technical assistance.

Declaration of interests: The authors declare that they have no known competing financial interests or personal relationships that could have appeared to influence the work reported in this paper.

References

[1] L. Hirsch, N. Jette, A. Frolkis, T. Steeves, T. Pringsheim, The Incidence of Parkinson's Disease: A Systematic Review and Meta-Analysis, Neuroepidemiology, 46 (2016) 292-300.
[2] E. Wollmer, S. Klein, A review of patient-specific gastrointestinal parameters as a platform for developing in vitro models for predicting the in vivo performance of oral dosage forms in patients with Parkinson's disease, Int J Pharm, 533 (2017) 298-314.
[3] A. Di Stefano, P. Sozio, A. Iannitelli, L.S. Cerasa, New drug delivery strategies for improved Parkinson's disease therapy, Expert Opin Drug Deliv, 6 (2009) 389-404.
[4] S. Di Gioia, A. Trapani, D. Mandracchia, E. De Giglio, S. Cometa, V. Mangini, F. Arnesano, G. Belgiovine, S. Castellani, L. Pace, M.A. Lavecchia, G. Trapani, M. Conese, G. Puglisi, T. Cassano, Intranasal delivery of

dopamine to the striatum using glycol chitosan/sulfobutylether-beta-cyclodextrin based nanoparticles, Eur J Pharm Biopharm, 94 (2015) 180-193.
[5] C. Rodriguez-Nogales, E. Garbayo, M.M. Carmona-Abellan, M.R. Luquin, M.J. Blanco-Prieto, Brain aging and Parkinson's disease: New therapeutic approaches using drug delivery systems, Maturitas, 84 (2016) 25-31.
[6] F. Re, M. Gregori, M. Masserini, Nanotechnology for neurodegenerative disorders, Maturitas, 73 (2012) 45-51.
[7] M. Conese, R. Cassano, E. Gavini, G. Trapani, G. Rassu, E. Sanna, S. Di Gioia, A. Trapani, Harnessing Stem Cells and Neurotrophic Factors with Novel Technologies in the Treatment of Parkinson's Disease, Curr Stem Cell Res Ther, 14 (2019) 549-569.
[8] C. Saraiva, C. Praca, R. Ferreira, T. Santos, L. Ferreira, L. Bernardino, Nanoparticle-mediated brain drug delivery: Overcoming blood-brain barrier to treat neurodegenerative diseases, J Control Release, 235 (2016) 34-47.
[9] G.H. Hawthorne, M.P. Bernuci, M. Bortolanza, V. Tumas, A.C. Issy, E. Del-Bel, Nanomedicine to Overcome Current Parkinson's Treatment Liabilities: A Systematic Review, Neurotox Res, 30 (2016) 715-729.
[10] S. Pillay, V. Pillay, Y.E. Choonara, D. Naidoo, R.A. Khan, L.C. du Toit, V.M. Ndesendo, G. Modi, M.P. Danckwerts, S.E. Iyuke, Design, biometric simulation and optimization of a nano-enabled scaffold device for enhanced delivery of dopamine to the brain, Int J Pharm, 382 (2009) 277-290.
[11] E. De Giglio, A. Trapani, D. Cafagna, L. Sabbatini, S. Cometa, Dopamine-loaded chitosan nanoparticles: formulation and analytical characterization, Anal Bioanal Chem, 400 (2011) 1997-2002.
[12] A. Trapani, E. De Giglio, D. Cafagna, N. Denora, G. Agrimi, T. Cassano, S. Gaetani, V. Cuomo, G. Trapani, Characterization and evaluation of chitosan nanoparticles for dopamine brain delivery, Int J Pharm, 419 (2011) 296-307.
[13] R. Pahuja, K. Seth, A. Shukla, R.K. Shukla, P. Bhatnagar, L.K. Chauhan, P.N. Saxena, J. Arun, B.P. Chaudhari, D.K. Patel, S.P. Singh, R. Shukla, V.K. Khanna, P. Kumar, R.K. Chaturvedi, K.C. Gupta, Trans-blood brain barrier delivery of dopamine-loaded nanoparticles reverses functional deficits in parkinsonian rats, ACS Nano, 9 (2015) 4850-4871.
[14] E.R. Rashed, H.A. Abd El-Rehim, M.A. El-Ghazaly, Potential efficacy of dopamine loaded-PVP/PAA nanogel in experimental models of Parkinsonism: possible disease modifying activity, J Biomed Mater Res A, 103 (2015) 1713-1720.
[15] V. Bourganis, O. Kammona, A. Alexopoulos, C. Kiparissides, Recent advances in carrier mediated nose-to-brain delivery of pharmaceutics, Eur J Pharm Biopharm, 128 (2018) 337-362.
[16] E. Samaridou, M.J. Alonso, Nose-to-brain peptide delivery - The potential of nanotechnology, Bioorg Med Chem, 26 (2018) 2888-2905.
[17] A. Trapani, D. Tricarico, A. Mele, F. Maqoud, D. Mandracchia, P. Vitale, V. Capriati, G. Trapani, V. Dimiccoli, A. Tolomeo, A. Scilimati, A novel injectable formulation of 6-fluoro-l-DOPA imaging agent for diagnosis of neuroendocrine tumors and Parkinson's disease, Int J Pharm, 519 (2017) 304-313.
[18] A. Trapani, D. Mandracchia, G. Tripodo, S. Cometa, S. Cellamare, E. De Giglio, P. Klepetsanis, S.G. Antimisiaris, Protection of dopamine towards autoxidation reaction by encapsulation into non-coated- or chitosan- or thiolated chitosan-coated-liposomes, Colloids Surf B Biointerfaces, 170 (2018) 11-19.
[19] H. Li, P. Yang, W. Knight, Y. Guo, J.S. Perlmutter, T.L.S. Benzinger, J.C. Morris, J. Xu, The interactions of dopamine and oxidative damage in the striatum of patients with neurodegenerative diseases, J Neurochem, 152 (2020) 235-251.
[20] A. Ancona, M. Sportelli, A. Trapani, R.A. Picca, C. Palazzo, E. Bonerba, F. Mezzapesa, G. Tantillo, G. Trapani, N. Cioffi, Synthesis and Characterization of Hybrid Copper-Chitosan Nano-antimicrobials by Femtosecond Laser-Ablation in Liquids, Material Letters, 136 (2014) 397-400.
[21] D. Mandracchia, A. Rosato, A. Trapani, T. Chlapanidas, I.M. Montagner, S. Perteghella, C. Di Franco, M.L. Torre, G. Trapani, G. Tripodo, Design, synthesis and evaluation of biotin decorated inulin-based polymeric micelles as long-circulating nanocarriers for targeted drug delivery, Nanomedicine, 13 (2017) 1245-1254.

[22] A. Singh, H.L. Kutscher, J.C. Bulmahn, S.D. Mahajan, G.S. He, P.N. Prasad, Laser ablation for pharmaceutical nanoformulations: Multi-drug nanoencapsulation and theranostics for HIV, Nanomedicine, 25 (2020) 102172.
[23] J. Garcia-Pardo, F. Novio, F. Nador, I. Cavaliere, S. Suarez-Garcia, S. Lope-Piedrafita, A.P. Candiota, J. Romero-Gimenez, B. Rodriguez-Galvan, J. Bove, M. Vila, J. Lorenzo, D. Ruiz-Molina, Bioinspired Theranostic Coordination Polymer Nanoparticles for Intranasal Dopamine Replacement in Parkinson's Disease, ACS Nano, 15 (2021) 8592-8609.
[24] M. Agrawal, S. Saraf, S.G. Antimisiaris, N. Hamano, S.D. Li, M. Chougule, S.A. Shoyele, U. Gupta, Ajazuddin, A. Alexander, Recent advancements in the field of nanotechnology for the delivery of anti-Alzheimer drug in the brain region, Expert Opin Drug Deliv, 15 (2018) 589-617.
[25] A. Trapani, V. Laquintana, A. Lopedota, M. Franco, A. Latrofa, G. Talani, E. Sanna, G. Trapani, G. Liso, Evaluation of new propofol aqueous solutions for intravenous anesthesia, Int J Pharm, 278 (2004) 91-98.
[26] G. Tripodo, G. Pasut, A. Trapani, A. Mero, F.M. Lasorsa, T. Chlapanidas, G. Trapani, D. Mandracchia, Inulin-D-alpha-tocopherol succinate (INVITE) nanomicelles as a platform for effective intravenous administration of curcumin, Biomacromolecules, 16 (2015) 550-557.
[27] T. Karamanidou, V. Bourganis, O. Kammona, C. Kiparissides, Lipid-based nanocarriers for the oral administration of biopharmaceutics, Nanomedicine, 11 (2016) 3009-3032.
[28] G. Kaur, M. Arora, M.N.V. Ravi Kumar, Oral Drug Delivery Technologies-A Decade of Developments, J Pharmacol Exp Ther, 370 (2019) 529-543.
[29] G. Trapani, M. Franco, A. Trapani, A. Lopedota, A. Latrofa, E. Gallucci, S. Micelli, G. Liso, Frog intestinal sac: a new in vitro method for the assessment of intestinal permeability, J Pharm Sci, 93 (2004) 2909-2919.
[30] A. Trapani, G. Tripodo, D. Mandracchia, N. Cioffi, N. Ditaranto, V. De Leo, H. Cordero, M.A. Esteban, Glutathione-loaded solid lipid nanoparticles based on Gelucire® 50/13: Spectroscopic characterization and interactions with fish cells, J Drug Deliv Sci Tech, 47 (2018) 359-366.
[31] A. Trapani, D. Mandracchia, G. Tripodo, S. Di Gioia, S. Castellani, N. Cioffi, N. Ditaranto, M.A. Esteban, M. Conese, Solid lipid nanoparticles made of self-emulsifying lipids for efficient encapsulation of hydrophilic substances, in: AIP Conference Proceedings, 2019, pp. 020004.
[32] A. Trapani, C. Palazzo, M. Contino, M.G. Perrone, N. Cioffi, N. Ditaranto, N.A. Colabufo, M. Conese, G. Trapani, G. Puglisi, Mucoadhesive properties and interaction with P-glycoprotein (P-gp) of thiolated-chitosans and -glycol chitosans and corresponding parent polymers: a comparative study, Biomacromolecules, 15 (2014) 882-893.
[33] S.G. Antimisiaris, Preparation of DRV Liposomes, Methods Mol Biol, 1522 (2017) 23-47.
[34] S. Cometa, M.A. Bonifacio, G. Trapani, S. Di Gioia, L. Dazzi, E. De Giglio, A. Trapani, In vitro investigations on dopamine loaded Solid Lipid Nanoparticles, J Pharm Biomed Anal, 185 (2020) 113257.
[35] A. Trapani, D. Mandracchia, C. Di Franco, H. Cordero, P. Morcillo, R. Comparelli, A. Cuesta, M.A. Esteban, In vitro characterization of 6-Coumarin loaded solid lipid nanoparticles and their uptake by immunocompetent fish cells, Colloids Surf B Biointerfaces, 127 (2015) 79-88.
[36] S. Perteghella, D. Mandracchia, M.L. Torre, R. Tamma, D. Ribatti, A. Trapani, G. Tripodo, Anti-angiogenic activity of N,O-carboxymethyl-chitosan surface modified solid lipid nanoparticles for oral delivery of curcumin, J. Drug Deliv. Sci. Technol., 56 (2020) 101494.
[37] D. Mandracchia, A. Trapani, S. Perteghella, M. Sorrenti, L. Catenacci, M.L. Torre, G. Trapani, G. Tripodo, pH-sensitive inulin-based nanomicelles for intestinal site-specific and controlled release of celecoxib, Carbohydr Polym, 181 (2018) 570-578.
[38] A. Trapani, L. Guerra, F. Corbo, S. Castellani, E. Sanna, L. Capobianco, A.G. Monteduro, D.E. Manno, D. Mandracchia, S. Di Gioia, M. Conese, Cyto/Biocompatibility of Dopamine Combined with the Antioxidant Grape Seed-Derived Polyphenol Compounds in Solid Lipid Nanoparticles, Molecules, 26 (2021).
[39] S.A. Pagar, D.M. Shinkar, R.B. Saudagar, Development and evaluation of in situ nasal mucoadhesive gel of metoprolol succinate by using 3^2 full factorial design, Int. J. Pharm. Pharm. Sci., 6 (2014) 218-223.
[40] R. Pellitteri, M. Spatuzza, A. Russo, S. Stanzani, Olfactory ensheathing cells exert a trophic effect on the hypothalamic neurons in vitro, Neurosci Lett, 417 (2007) 24-29.
[41] T. Musumeci, R. Pellitteri, M. Spatuzza, G. Puglisi, Nose-to-brain delivery: evaluation of polymeric nanoparticles on olfactory ensheathing cells uptake, J Pharm Sci, 103 (2014) 628-635.

[42] S. Castellani, A. Trapani, A. Spagnoletta, L. di Toma, T. Magrone, S. Di Gioia, D. Mandracchia, G. Trapani, E. Jirillo, M. Conese, Nanoparticle delivery of grape seed-derived proanthocyanidins to airway epithelial cells dampens oxidative stress and inflammation, J Transl Med, 16 (2018) 140.
[43] S. Rossi, F. Ferrari, M.C. Bonferoni, C. Caramella, Characterization of chitosan hydrochloride-mucin interaction by means of viscosimetric and turbidimetric measurements, Eur J Pharm Sci, 10 (2000) 251-257.
[44] D. Ivarsson, M. Wahlgren, Comparison of in vitro methods of measuring mucoadhesion: ellipsometry, tensile strength and rheological measurements, Colloids Surf B Biointerfaces, 92 (2012) 353-359.
[45] L. Becker Peres, P.H.H. de Araujo, C. Sayer, Solid lipid nanoparticles for encapsulation of hydrophilic drugs by an organic solvent free double emulsion technique, Colloids Surf B Biointerfaces, 140 (2016) 317-323.
[46] N. Matougui, L. Boge, A.C. Groo, A. Umerska, L. Ringstad, H. Bysell, P. Saulnier, Lipid-based nanoformulations for peptide delivery, Int J Pharm, 502 (2016) 80-97.
[47] M.C. Woodle, Surface-modified liposomes: assessment and characterization for increased stability and prolonged blood circulation, Chem Phys Lipids, 64 (1993) 249-262.
[48] E. Ortega, S. Blanco, A. Ruiz, M.A. Peinado, S. Peralta, M.E. Morale, Lipid nanoparticles for the transport of drugs like dopamine through the blood-brain barrier, J Nanoparticle Res, 23 (2021) 106.
[49] C. Palazzo, G. Trapani, G. Ponchel, A. Trapani, C. Vauthier, Mucoadhesive properties of low molecular weight chitosan- or glycol chitosan- and corresponding thiomer-coated poly(isobutylcyanoacrylate) core-shell nanoparticles, Eur J Pharm Biopharm, 117 (2017) 315-323.
[50] M.I. Adamczak, E. Hagesaether, G. Smistad, M. Hiorth, An in vitro study of mucoadhesion and biocompatibility of polymer coated liposomes on HT29-MTX mucus-producing cells, Int J Pharm, 498 (2016) 225-233.
[51] G. Tripodo, A. Trapani, A. Rosato, C. Di Franco, R. Tamma, G. Trapani, D. Ribatti, D. Mandracchia, Hydrogels for biomedical applications from glycol chitosan and PEG diglycidyl ether exhibit pro-angiogenic and antibacterial activity, Carbohydr Polym, 198 (2018) 124-130.
[52] D. Mandracchia, A. Trapani, G. Tripodo, M.G. Perrone, G. Giammona, G. Trapani, N.A. Colabufo, In vitro evaluation of glycol chitosan based formulations as oral delivery systems for efflux pump inhibition, Carbohydr Polym, 166 (2017) 73-82.
[53] E.B. Souto, J.F. Fangueiro, R.H. Müller, Solid Lipid Nanoparticles (SLN™), in: I.F. Uchegbu, A.G. Schätzlein, W.P. Cheng, A. Lalatsa (Eds.) Fundamentals of Pharmaceutical Nanoscience, Springer, New York, NY, 2013, pp. 91-116.
[54] H. Yuan, C.Y. Chen, G.H. Chai, Y.Z. Du, F.Q. Hu, Improved transport and absorption through gastrointestinal tract by PEGylated solid lipid nanoparticles, Mol Pharm, 10 (2013) 1865-1873.
[55] A. Gordillo-Galeano, C.E. Mora-Huertas, Solid lipid nanoparticles and nanostructured lipid carriers: A review emphasizing on particle structure and drug release, Eur J Pharm Biopharm, 133 (2018) 285-308.
[56] D. Wang, Y. Peng, Y. Xie, B. Zhou, X. Sun, R. Kang, D. Tang, Antiferroptotic activity of non-oxidative dopamine, Biochem Biophys Res Commun, 480 (2016) 602-607.
[57] M.A. Mena, V. Davila, D. Sulzer, Neurotrophic effects of L-DOPA in postnatal midbrain dopamine neuron/cortical astrocyte cocultures, J Neurochem, 69 (1997) 1398-1408.
[58] G.C. O'Keeffe, P. Tyers, D. Aarsland, J.W. Dalley, R.A. Barker, M.A. Caldwell, Dopamine-induced proliferation of adult neural precursor cells in the mammalian subventricular zone is mediated through EGF, Proc Natl Acad Sci U S A, 106 (2009) 8754-8759.
[59] Y. Yu, Z. Pang, W. Lu, Q. Yin, H. Gao, X. Jiang, Self-assembled polymersomes conjugated with lactoferrin as novel drug carrier for brain delivery, Pharm Res, 29 (2012) 83-96.
[60] D. Manzanares, V. Cena, Endocytosis: The Nanoparticle and Submicron Nanocompounds Gateway into the Cell, Pharmaceutics, 12 (2020).
[61] L. Arana, L. Bayon-Cordero, L.I. Sarasola, M. Berasategi, S. Ruiz, I. Alkorta, Solid Lipid Nanoparticles Surface Modification Modulates Cell Internalization and Improves Chemotoxic Treatment in an Oral Carcinoma Cell Line, Nanomaterials (Basel), 9 (2019).
[62] A.S. Al Khafaji, M.D. Donovan, Endocytic Uptake of Solid Lipid Nanoparticles by the Nasal Mucosa, Pharmaceutics, 13 (2021).
[63] J.J. Rennick, A.P.R. Johnston, R.G. Parton, Key principles and methods for studying the endocytosis of biological and nanoparticle therapeutics, Nat Nanotechnol, 16 (2021) 266-276.

[64] M. Maugeri, M. Nawaz, A. Papadimitriou, A. Angerfors, A. Camponeschi, M. Na, M. Holtta, P. Skantze, S. Johansson, M. Sundqvist, J. Lindquist, T. Kjellman, I.L. Martensson, T. Jin, P. Sunnerhagen, S. Ostman, L. Lindfors, H. Valadi, Linkage between endosomal escape of LNP-mRNA and loading into EVs for transport to other cells, Nat Commun, 10 (2019) 4333.
[65] E. Samaridou, J. Heyes, P. Lutwyche, Lipid nanoparticles for nucleic acid delivery: Current perspectives, Adv Drug Deliv Rev, 154-155 (2020) 37-63.
[66] C.P. Costa, J.N. Moreira, J.M. Sousa Lobo, A.C. Silva, Intranasal delivery of nanostructured lipid carriers, solid lipid nanoparticles and nanoemulsions: A current overview of in vivo studies, Acta Pharm Sin B, 11 (2021) 925-940.
[67] M. Agrawal, S. Saraf, S. Saraf, S.G. Antimisiaris, M.B. Chougule, S.A. Shoyele, A. Alexander, Nose-to-brain drug delivery: An update on clinical challenges and progress towards approval of anti-Alzheimer drugs, J Control Release, 281 (2018) 139-177.

Captions to Figures

Fig. 1. TEM micrographs of DA-SLN (SLN 1, panels a, b from Ref 38) and GCS-DA-SLN (SLN 2, panel c).

Fig. 2. a) Particle size changes over the time of SLN incubated for 8 weeks at 4°C; b) DA content changes over the time after storage of SLN at 4 °C for 8 weeks. Each experiment was performed in triplicate and the results are expressed as mean ± standard deviation of each mean. Blue bars refer to incubation of SLN 1 and red bars refer to SLN 2. For all sample sets, the value referring to time zero was taken as control. ** $p < 0.001$ *vs* control. (For interpretation of the references to colour in this Fig. legend, the reader is referred to the web version of this article).

Fig. 3. Mucoadhesive properties in SNF of a) Lip 1 (green), Lip 2 (black), SLN 1 (blue) and SLN 2 (red). HEC (magenta) was taken as positive control. (For interpretation of the references to colour in this Fig. legend, the reader is referred to the web version of this article).

Fig. 4. C1s curve fittings of DA (a), GCS (b), Gelucire 50/13 (c) and Tween 85 (d) and formulations (plain SLN (e) and SLN 2 (f)). Uncertainty on BE peak positions was ±0.2 eV.

Fig. 5. Cytotoxicity of SLN derivatives. OECs were challenged with plain-SLN (a) for 24 h at the indicated concentrations (μg/mL). SLN 1 (b) and SLN 2 (c) were used at the same lipid concentrations, resulting in DA as 0.45, 0.9, 1.8, 4.5, 9.0 and 18 μM. Cells were then assayed for vitality by the MTT assay. Controls (CTRL) are untreated cells (100% of vitality), whereas 1% Triton X-100 (TX) was used as positive control. **p<0.05; ***p < 0.0001 *vs* CTRL. Data are the results of two-three experiments each carried out in four wells.

Fig. 6. Cytotoxicity of liposomal formulations. OECs were challenged with Lip1 (a) and Lip2 (b) for 24 h at the indicated concentrations (μg/mL), obtaining DA concentrations of 0.3, 1.17, 4.7, 9.0 and 18.75, and 75 μM. Cells were then assayed for vitality by the MTT assay. Controls (CTRL) are untreated cells (100% of vitality), whereas 1% Triton X-100 (TX) was used as positive control. ***p < 0.0001 *vs* CTRL. Data are the results of two experiments each carried out in four wells.

Fig. 7. Cellular uptake of FITC-SLN 2 by OECs. OECs were incubated with the indicated concentrations (μg/mL) of FITC-SLN 2 for 24 h and evaluated by flow cytometry. Positive cells, shown as percentages (a), and the mean fluorescence intensity (b), were obtained in three experiments each conducted in triplicate. In a) **p<0.001 and ***p<0.0001 (in black) denote differences between 0.25 *vs* 1.0, 2.5, 5.0 and 10.0; *p<0.05, **p<0.001 and ***p<0.0001 (in gray) denote differences between 1.0 *vs* 2.5, 5.0 and 10.0. In b) **p<0.001 denotes differences between 0.25 and 10; *p<0.05 denotes differences between 1.0 and 2.5 *vs* 10.0.

Fig. 8. Cellular uptake of FITC-liposomal formulations by OECs. OECs were incubated with the indicated concentrations (μg/mL) of Lip1 (a, b) or Lip 2 (c, d) for 24 h and evaluated by flow cytometry. Positive cells, shown as percentages (A, C), and the mean fluorescence intensity (b, d), were obtained in two experiments each conducted in triplicate. In A) *p<0.05 denote differences between 0.25 and 1 *vs* 64. In b) *p<0.05 denotes differences between 0.25 *vs* 16. In c), **p<0.001 denotes differences between 0.25 *vs* 4 and 16, while ***p<0.0001 between 0.25 *vs* 64. In d), *p<0.05 denote differences between 0.25 *vs* 4.

Fig. 9. Schematic representation of the a) PEGylated SLN 1; b) PEGylated SLN 2.

Fig. 1S. C1s signal relevant to GCS-SLN

Fig. 2S. C1s signal relevant to DA-GCS-SLN

Table 1. Particle size, polydispersity index (PDI), zeta potential values, encapsulation efficiency of different formulations prepared.

Formulation	Size (nm)	PDI	Zeta Potential	Encapsulation (E.E.%)	Ref.
DA-loaded Liposomes					
Uncoated (Lip 1)	172 ± 2	0.27±0.02	-10.8 ± 1.0	5.2 ± 0.3	[18]
CS-GSH-coated [a] (Lip 2)	146 ± 4	0.16±0.01	+1.5 ± 0.0	12.2 ± 0.3	[18]
6-COUM Uncoated (6-COUM Lip 1)	190 ± 5	0.36±0.02	-9.7 ± 0.5		
6-COUM CS-GSH-coated (6-COUM Lip 2)	161 ± 12	0.25±0.01	+1.9 ± 0.4		
DA-loaded Gelucire® 50/13 based SLN					
DA-SLN (SLN 1)	171±6	0.2±0.01	-2.0±0.7	19±3	[33]
GCS-DA-SLN (SLN 2)	147±24	0.5±0.07	+5.2±1.7	81±2	[33]
Control SLN					
Plain SLN	141±11	0.34±0.06	−9.7 ± 0.8		[30]
GCS-SLN	265±5	0.49±0.04	+8.5±0.6		[30]
FITC-SLN 2	268 ± 9	0.5 ± 0.05	+15.2 ± 0.2		

[a]CS-GSH/lipids weight ratio = 0.3.

Table 2: Atomic percentages of the elements present on the surface of the bare constituents and on the SLN, with or without DA and/or GCS.

Sample	**Atomic percentage %**					
	C1s	O1s	N1s	Cl2p	Na1s	Si2p
DA	71.7	15.3	6.8	6.1	--	--
GCS	61.2	31.2	6.2	--	1.5	--
Gelucire 50/13	86.7	13.3	--	--	--	--
Tween 85	71.8	26.6	--	--	--	1.6
Plain SLN	85.4	14.6	--	--	--	--
GCS-SLN	65.6	25.5	--	--	--	8.8
DA-SLN (SLN 1)	69.4	24.6	0.4	0.2	--	5.4
GCS-DA-SLN (SLN 2)	74.0	21.2	0.5	0.3	--	4.1